UPTEC X 01 001
JAN 2001

ISSN 1401-2138

HENRIK SJÖLANDER

Fluorescent and electrophysiological study of a hyperpolarization-activated ion channel

Master’s degree project

Molecular Biotechnology Programme
Uppsala University School of Engineering

UPTEC X 01 001	**Date of issue 2001-01**

Author

Henrik Sjölander

Title (English)

Fluorescent and electrophysiological study of a hyperpolarization-activated ion channel

Title (Swedish)

Abstract

The gating mechanism of the hyperpolarization-activated cyclic nucleotide-gated potassium channel SPIH was studied. Membrane impermeable reagents were used to probe external accessibility of introduced cysteines in the voltage sensor of SPIH. The interpretation of these data is that the sensor undergoes a voltage dependent transmembrane movement. A voltage clamp fluorometry technique was used to correlate this movement of the sensor to the opening of the channel. Together these data lead to a new hypothesis of the gating mechanism for SPIH. The channel is closed at positive potentials, when the voltage sensor is in its outermost position. Stepping to negative voltages leads to an inward movement of the sensor that triggers opening of the channel, resulting in an inward current.

Keywords

SPIH, HCN, hyperpolarization, channel, potassium, gating mechanism

Supervisors

Peter Larsson

Nobel Institute for Neurophysiology, Department of Neuroscience, Karolinska Institutet

Examiner

Fredrik Elinder

Nobel Institute for Neurophysiology, Department of Neuroscience, Karolinska Institutet

Project name	Sponsors
Language **English**	Security
ISSN 1401-2138	Classification
Supplementary bibliographical information	Pages **35**

Biology Education Centre Biomedical Center Husargatan 3 Uppsala
Box 592 S-75124 Uppsala Tel +46 (0)18 4710000 Fax +46 (0)18 555217

Fluorescent and electrophysiological study of a hyperpolarization-activated ion channel

Henrik Sjölander

Sammanfattning

Rytmer finns i många former i naturen, växlingen mellan årstider samt natt och dag tillhör de mest påtagliga exemplen. Rytmer finns även i levande organismer, tänk bara på andningen och hjärtats regelbundna slag. Dessa kroppsliga rytmer har sitt ursprung i elektriska strömmar in i och ut från kroppens celler. Strömmarna består av laddade partiklar, joner, som vandrar genom speciella kanaler i cellerna. I detta examensarbete har öppnings-/stängningsmekanismen hos en sådan kanal studerats.

Elektrofysiologiska mätningar visar att ett segment hos kanalen, kallad spänningssensorn, rör sig genom cellens membran vid olika spänningar. Med hjälp av fluorescensförsök kunde rörelsen hos spänningssensorn kopplas till öppnandet av kanalen. Med bakgrund av dessa data förslås en ny hypotes för öppnings-/stängningsmekanismen hos kanalerna.
Vid positiva potentialer återfinns spänningssensorn i ett yttre läge och kanalen är stängd. Om man ändrar spänningen över membranet så att insidan av cellen blir negativ i förhållande till utsidan, kommer sensorn att dras in i membranet vilket leder till öppnandet av kanalen och joner kan börja vandra in i cellen.

Den här mekanismen har hittills ej varit känd för rytmreglerande kanaler, men eftersom kanalerna reglerar fundamentala och livsviktiga processer i våra kroppar är kunskapen om öppnings-/stängningsmekanismen av största vikt för att kunna förstå och bota hjärtrelaterade och neurologiska sjukdomar. Detta examensarbete kan ses som ett första steg till en djupare förståelse av rytmreglerande kanaler.

Examensarbete 20 p i Molekylär bioteknikprogrammet
Uppsala universitet, januari 2001

Contents

1. Introduction **2**

2. Background **3**

2.1. Classification and Structure of Potassium Channels **3**

2.1.1. 2TM Inward Rectifier K^+ Channels *5*

2.1.2. 6TM K^+ Channels *6*

2.2. Physiology of Two 6TM Inward Rectifier K^+ Channels **7**

2.2.1. HERG K^+ Channel *7*

2.2.2. HCN K^+ Channels *7*

2.3. Gating Mechanism of Three 6TM K^+ Channels **9**

2.3.1. Gating Mechanism of the Shaker *K^+ Channel* *9*

2.3.2. Gating Mechanism of the HERG K^+ Channel *13*

2.3.3. Gating Mechanism of HCN K^+ Channels *14*

3. Materials and Methods **16**

3.1. Solutions **16**

3.2. Molecular Biology **17**

3.2.1. Site-Directed Mutagenesis *17*

3.2.2. Transcription *17*

3.3. Expression of SPIH Channels **18**

3.4. Electrophysiology **18**

3.4.1. Two-Electrode Voltage Clamp *18*

3.4.2. MTSET/MTSES Labeling *19*

3.5. Voltage Clamp Fluorometry **19**

4. Results and Discussion **20**

4.1. Electrophysiological Measurements of SPIH wild-type and Mutant Channels **20**

4.2. Permeability **22**

4.3. cAMP regulation **23**

4.4. Transmembrane Movement of the Voltage Sensor of SPIH Channels **24**

4.5. Voltage Clamp Fluorometry **28**

5. Conclusions **30**

6. Acknowledgements **32**

7. References **33**

1. Introduction

Rhythms exist in various forms in nature, the change of seasons and day and night are just a few examples. Rhythms are also found in living creatures in the form of the regular beating of the heart, the sleep-cycle and the respiratory rhythms. These 'physical rhythms' are to some extent all regulated by electric currents of ions (Dekin, 1993; DiFrancesco, 1993; McCormick & Bal, 1997). These currents flow into and out from special cells via ion channels in the cell membrane. Some of the channels responsible for rhythms belong to a group of voltage-activated potassium channels, called hyperpolarization-activated cyclic nucleotide-gated potassium channels (HCN) (Clapham, 1998).

This recently cloned group of voltage-activated channels has several interesting properties that distinguish them from other related channels. Contrary to the majority of potassium channels the HCNs are activated at negative and not at positive voltages. The current of HCNs is normally inward and is carried not only by potassium but also by sodium ions, whereas other voltage-activated K^+ channels have an outward current of almost exclusively potassium ions. In contrast to related channels the HCNs, as the name indicates, are regulated by cyclic nucleotides. Although all these different features between HCNs and other voltage-activated potassium channels, they have fairly similar protein sequence (Santoro & Tibbs, 1999) and are likely to have the same overall structure (Ludwig *et al.*, 1999).

The differences between HCNs and related potassium channels concerning the gating mechanisms, opening, closure and inactivation, have not yet been completely explained although possible explanations have been given (Miller & Aldrich, 1996; Clapham, 1998). The aim of this master's degree project was to characterize a special HCN found in a species of sea urchins, *Strongylocentrotus purpuratus*, called SPIH (Gauss *et al.*, 1998) and try to describe the gating mechanism of the channel. This was done by following the movement of the voltage sensor of the channel at different potentials using two different methods: 1) a fluorescent technique, which probes molecular rearrangement around the sensor and 2) a technique that probes external accessibility of introduced cysteines in the sensor using membrane impermeable reagents. In the fluorescence experiments a flourophore, whose fluorescence is sensitive to its local environment, is coupled to the voltage sensor. By combining fluorescence measurements with voltage clamping, a technique in which the current at fixed potentials is measured, the gating conformational changes could be followed in real time and a correlation between sensor movement and channel opening could be obtained.

The results indicate that the voltage sensor undergoes an outward movement at positive voltages and is pulled back into the membrane at negative potentials. This is consistent with similar experiments with the *Shaker* K^+ channel, a related voltage-activated channel (Larsson *et al.*, 1996), but no results of voltage sensor movement of HCN channels has until now been published. The fluorescent experiments indicate that there is a correlation between the movement of the sensor and opening of the channels and that an inward

movement of the voltage sensor must precede opening of the channel. Taken together these results indicate that the gating mechanism of SPIH differs from the mechanism of the well-characterized *Shaker* channel. I propose that the SPIH channel is closed at positive voltages when the voltage sensor is in its outermost position. At negative voltages the sensor is pulled into the membrane and this triggers opening of the activation gate and an inward current flows through the channel. After a short while, a few tens of milliseconds, the current ceases due to closure of another gate, the inactivation gate. A step back to positive voltages leads to opening of the inactivation gate. The channel is once again open and currents can now move through the channel again but now in an outward direction. This current stops after some milliseconds due to deactivation that is closure of the activation gate. Then the sensor moves outward and the channel is now back in the closed state that it started from.

Knowledge of this gating mechanism of the HCN channels is very important since the channels are involved in fundamental processes in our bodies, such as respiratory and beating of the heart. This Master's degree project can be seen as a first step in the process of characterizing the HCNs and the knowledge might, in the future, provide a new tool for the discovery of pharmacological agents that are useful in treating cardiac and neurological diseases.

2. Background

2.1. Classification and Structure of Potassium Channels

Potassium channels were originally identified as the molecular structures that mediated the flow of potassium ions across the membrane of nerve cells during the course of events of an action potential. Today more insight in their diverse rolls is beginning to emerge. Besides involvement in terminating the action potentials in electrically excitable cells, K^+ channels play crucial roles in the intracellular K^+ recycling required for electrolyte balance in renal epithelium.Mitogenesis and proliferation in the immune response of B and T cells are dependent on hyperpolarization of the cells via K^+ channels. The electrical tuning of mechanosensory cells in auditorytransduction relies centrally on the gating kinetics of potassium channels (Miller, 2000). This is just a few examples of mechanism where these channels play a major part. This diversity of function of the channels is the cause for finding them in virtually all types of cells in all fully sequenced genomes, both eukaryotic, eubacterial and archael (Littleton & Ganetzky, 2000). No other ion channel type displays such ubiquity.

Many different subfamilies of K^+ channel are known today. The different families are divided based roughly on the physiological signals that control channel opening (Miller, 2000): voltage-activated, Ca^{2+}-activated, G-protein regulated and polyamine regulated are just a few examples.

There are two broad classes of K^+ channels defined by their transmembrane topology: the six-transmembrane-helix, 6TM, and the two-transmembrane-helix inward-rectified, 2TM, subtypes.

Although quite different topology both subtypes of channels consist of four identical or similar subunits that, by combining into a tetramer, constitute the channel (MacKinnon, 1991). The pore of the channel and the selectivity sequence, leading to specificity for potassium ions, are structural moieties that are common to both subtypes. The signature sequence reads, with minor deviations, TMxTVGYG, using single-letter amino acid code. Structural information of these parts of the channel is well known today since the structural determination of the bacterial KcsA channel (Doyle *et al.*, 1998). In figure 1 an extracellular view of the KcsA potassium channel is presented, showing the tetrameric organization of the four subunits with the pore of the channel.

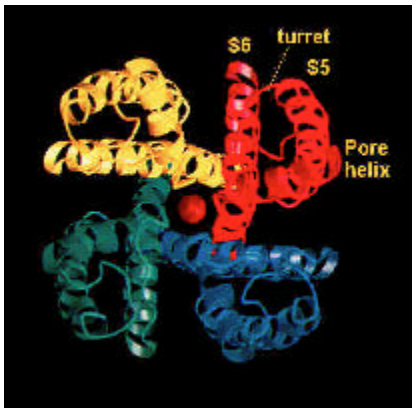

Figure 1. A ribbon representation illustrating the three-dimensional fold of the KcsA tetramer viewed from extracellular side. The four identical subunits are distinguished by color and the two transmembrane helices of one subunit are shown, S5 and S6 in *Shaker* nomenclature. A potassium ion can be seen colored red in the middle of the pore. Modified from Doyle *et al.*, 1998.

The KcsA belongs to the two-transmembrane-helix subtype and the two helices are indicated in the figure. The pore is easily seen as the hole in the middle of the channel, in figure 1 filled with a potassium ion. The mostcarboxy-terminal transmembrane helix, S6 in figure 1, and the selectivity sequence form most of the lining of the aqueous pore and thus carry the structural determinants of the high K^+ selectivity exhibited by most K^+ channels. The narrowest part of the pore, the selectivity filter, see figure 2, is a 3 Å diameter tube originating abruptly on the extra cellular side of the channel and extending normal to the membrane plane for about 10-15 Å. The wall of this structure is uncharged but highly hydrophilic, lined by twelve carbonyl groups, three from each subunit. The pore then widens to a 10 Å wide spherical water-filled cavity.

Resolving the structure of the KcsA channel has enabled an explanation of the ion selectivity and the high throughput rate of K^+ channel. Two distinct features of the pore are responsible for these phenomena: the precise coordination of dehydrated potassium ions by the channel and multiple ion occupancy within the permeation pathway (Miller 2000). The channel pore presents electronegative oxygen moieties arranged as a cage into which a dehydrated potassium ion fits exactly, but in which a sodium ion would fit so loosely that it energetically prefers to remain hydrated in the aqueous solution. This explains the high selectivity for K^+ of the channels compared to other ions. Another feature of the K^+ channel is the high rate of ion-flow through the pore. To achieve this high flow-rate the dissociation rate of the bound ion must be fast. Three ion-binding sites

located in a single file within the pore accomplish this. The sites are close enough that the ions electrostically repel each other, thereby causing the high flow-rate.

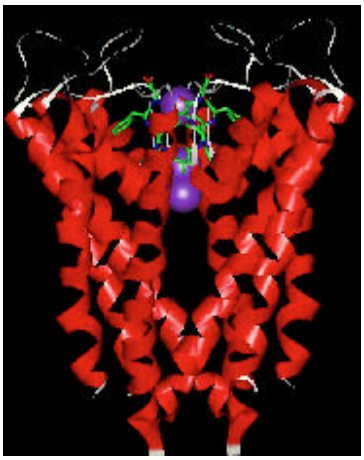

Figure 2. A ribbon presentation of the KcsA tetramer from another perspective, perpendicular to that in figure 1. The amino acids GYG of the selectivity filter are shown in sticks together with three coordinated potassium ions. From Kriksunov, 1998.

2.1.1. 2TM Inward Rectifier K^+ Channels

Three independent groups (Dascal *et al.*, 1993; Ho *et al.*, 1993; Kubo *et al.*, 1993) cloned, in 1993, the first 2TM inward rectifier K^+ channel, which was named Kir. Today several Kir channels have been cloned and classified into six subfamilies. Although they are closely related differences exist in, among others, the degree of rectification, phosphorylation and inhibition of ATP. The channels are found in a wide range of tissues from the heart and nervous system (Ishii *et al.*, 1994; Perier *et al.*, 1994) to kidneys (Ho *et al.*, 1993).

This family, as the name indicates, only contains two transmembrane helices per subunit, figure 3. The pore and selectivity filter are located between these two segments as for the bacterial KcsA channel in figure 1 and 2.

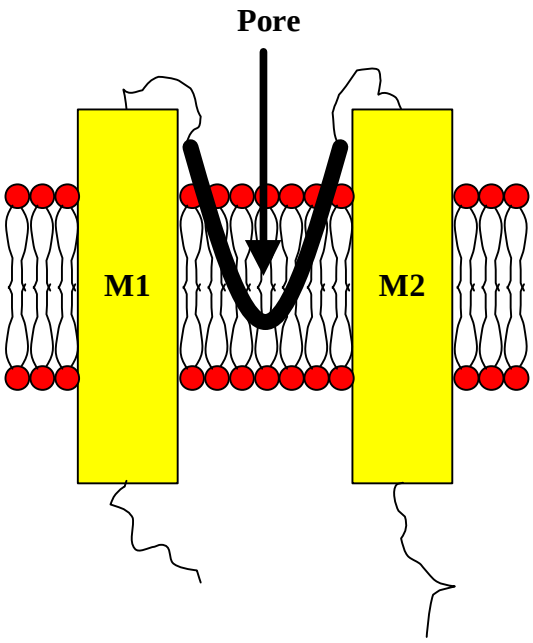

Figure 3. A schematic drawing of one subunit of a 2TM inward rectifier K^+ channel. The two transmembrane segments, marked M1 and M2, correspond to S5 and S6 in figure 1. The pore is indicated between the two helices.

The Kir channels are closed at positive voltages due to a pore block. At negative potentials the channels open through release of the block. This block consists of intracellular Mg^{2+} or polyamines. These positively charged substances block the channels in a voltage dependent manner leading to the inward rectifying properties of Kir. The block by polyamines and especially Mg^{2+} is strongly dependent on the external K^+ concentration, K_o, (Nichols & Lopatin, 1997). Increasing K_o relieves the block leading to less rectification. This effect is explained by binding of potassium ions at external sites and thereby knocking-off Mg^{2+} and polyamines from sites deeper inside the pore.

2.1.2. 6TM K^+ Channels

The most known and characterized potassium channel, the *Shaker* K^+ channel from *Drosophila*, belongs to the family of 6TM potassium channels. Most of what is known today about this family of channels has come from studies of the *Shaker* channel. This channel belongs to a group of depolarization-activated K^+ channels, but other groups such as the hyperpolarization-activated cyclic nucleotide-gated K^+ channels (HCN) also belong to this family.

The major difference of this family of channels compared to the 2TM K^+ channel family is the four extra transmembrane segments, S1-S4 in figure 4.

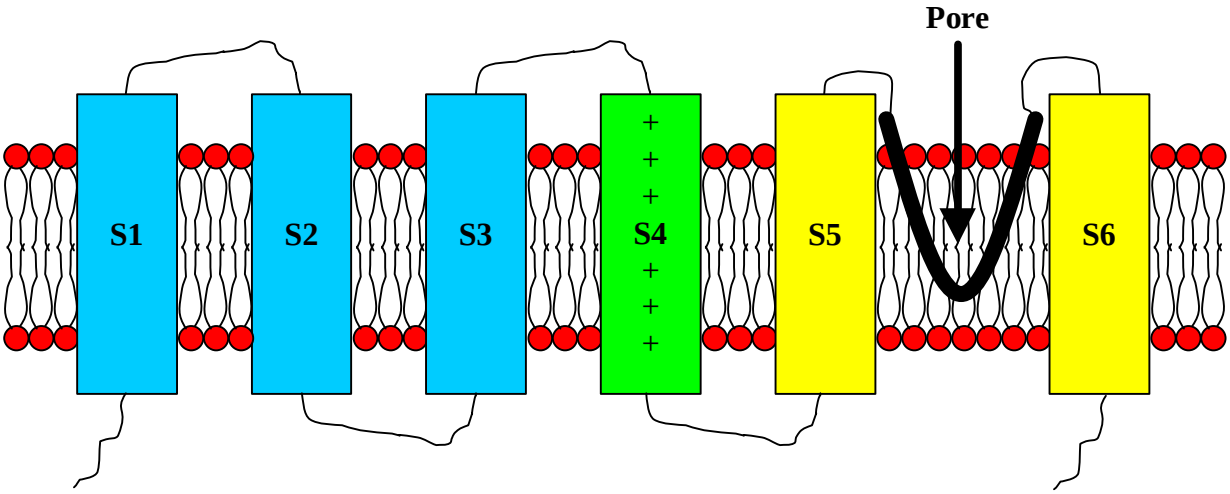

Figure 4. Schematic picture of one of the subunits of a six-transmembrane-helix voltage-gated K^+ channel. The two segments that correspond to the two helices of Kir and KcsA are labled S5 and S6. The positively charged amino acids in the voltage sensor, S4, are marked with +. The pore is shown between S5 and S6.

The four extra helices constitute the voltage-dependent domain of these channels, with a voltage sensor in the form of S4 (Liman *et al.*, 1991; Papazian *et al.*, 1991). This helix is responsible for the voltage-dependent activation of the channels. The segment consists of several positively charged amino acids at every third position. By containing charged residues S4 is able to respond to changes in the potential over the membrane. The number of positive charges and their relative position in S4 differs between different channels: *Shaker* contains seven positive charges at every third position whereas the HCNs have one or two more charges and also have one uncharged serine in the middle of sequence of the positive amino acids. Segment S1 to S3 are believed to stabilize the voltage sensor via electrostatic interactions between the positive charges in S4 and negatively charged residues in S2 and S3 (Papazian *et al.*, 1995).

2.2. Physiology of Two 6TM Inward Rectifier K^+ Channels

Three different groups of 6TM K^+ channels will be described in this project. Apart from the *Shaker* channel in *Drosophila* that has been mentioned above two inward rectifier 6TM channels, the HERG and HCN, will be characterized, to point out the differences of these channels in, above all, the gating mechanism.

2.2.1. HERG K^+ Channel

The HERG K^+ channel is found in cells in the heart of mammals. There it is involved in regulating cardiac rhythms. Several genetic defects in the gene coding for HERG is associated with 'long Q-T syndrome', an abnormality of cardiac rhythm involving the repolarization of the action potential (Curran *et al.*, 1995). The HERG K^+ channel is unusual in that it has the architectural plan of a 6TM voltage-gated channel, yet it exhibits rectification like that of the 2TM inward rectifier channels. This special feature of HERG will be explored in the section of gating mechanisms.

2.2.2. HCN K^+ Channels

Hyperpolarization-activated cyclic nucleotide-gated K^+ channels are a group of channels belonging to the family of 6TM voltage-gated channels. This group has a very special function in living organisms: they control rhythms. Different HCN channels are involved in regulating the respiratory rhythms, the sleep-cycle and the beating of the heart (Dekin, 1993; DiFrancesco, 1993; McCormick & Bal, 1997). They also have other important functions, such as synchronizing the activity of neuronal population (Maccaferri & McBain, 1996) and contributing to presynaptic facilitation of transmitter release (Beaumont & Zucker, 2000).

The HCN group has some features that differ them other channels in the 6TM K^+ channel family: activation at hyperpolarized potentials, permeable to both potassium and sodium and containing a cyclic nucleotide-binding domain (Clapham, 1998).

Just as the HERG and Kir channels the HCNs are activated at negative voltages. The opening of the channel at these potentials results in an inward mixed current,consisting

of both potassium and sodium ions. This is in contrast to other groups of potassium channels that usually have much larger selectivity of K^+ over Na^+. The cause of this might be changes in the amino acid sequence of the pore and the selectivity filter between the HCN channels and other K^+ channels, such as *Shaker*, see figure 5.

```
SPIH    416-TWALFKALSHMLCIGYGKFPPQS-438
HCN2    388-SFALFKAMSHMLCIGYGRQAPES-410
SHAKER  418-PDAFWWAVVTMTTVGYGDMTPVG-440
```

Figure 5. Comparison of the pore motif of SPIH with that of other channels. HCN2, the HAC1 channel found in the heart and brain of mammals (Ludwig *et al.*, 1998), *Shaker*, K^+ channels encoded by *Drosophila Shaker* B gene. Residues identical between all channels in bold and between SPIH and HCN2 in green. In *Shaker* K^+ channels the GYG sequence precedes a negatively charged aspartic acid, labeled red, whereas in SPIH and HCN2 positively charged residues are found in this position, labeled blue.

In the *Shaker* K^+ a negatively charged aspartic acid is found after the GYG sequence, whereas in HCN channels a postively residue is found in this position. Upstreams of GYG several threonines are positioned, which are absent in the HCN channels that even have a positive residue, a histidine, in this region of the pore. The loss of selectivity for the HCN channels is probably a consequence of these changes in amino acid sequence, which might make the pore smaller so it now can energetically coordinate both unhydrated Na^+ and K^+.

The HCNs are regulated by intracellular cAMP through the cyclic nucleotide-binding domain. Experiments have shown that it is the direct binding of cAMP to this domain that affects the channel (Gauss *et al.*, 1998). Binding of the nucleotide leads to increased ion flow through the channel. In the SPIH channel, a HCN found in sea urchins, the increase in inward current after cAMP treatment is due to increased open probability and prevention from undergoing inactivation (Gauss *et al.*, 1998). Another cAMP-dependent effect is seen for HCNs in mouse and humans, where the cyclic nucleotide shifts the activation of the channels to more positive voltages (Ludwig *et al.*, 1999). Although the mechanisms seem to be different the result is the same: increased current through the channels.

The HCNs are located in several tissues but they where first detected in the heart, where they regulate the cardiac rhythm. In the heart they are found in the sinus nodes, the Purkinje fibers and in ventricular and atrial muscles. In figure 6 a typical sequence of action potentials is shown, indicating the temporal position of the current from HCNs relative the action potential. First a slight depolarization over the threshold leads to opening of sodium and T-type calcium channels. The depolarization continues until these channels close and slower depolarization-activated potassium channels open. The K^+ current hyperpolarizes the cell and at some voltage the HCN channels start to open. The mixed K^+/Na^+ current, I_h, I_f or I_q in figure 6, contributes to the slow phase of depolarization that follows the hyperpolarization phase of an action potential.

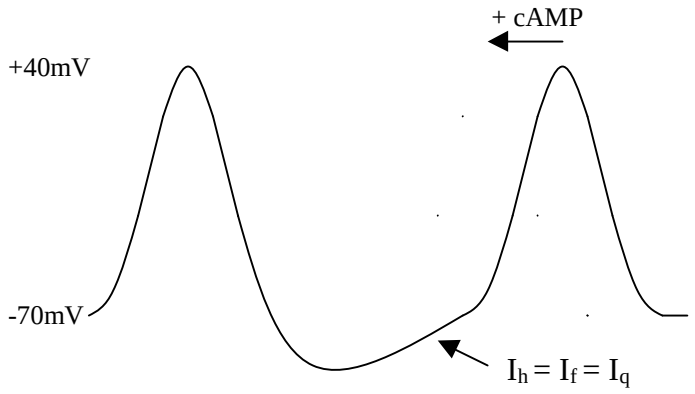

Figure 6. Contribution of the HCN current, named I_h, I_f of I_q in the literature, to the depolarization phase following repolarization after an action potential. cAMP increases the HCN current and thereby increasing depolarization, leading to shorter time between two action potentials.

Sympathetic stimulation in the body leads to release of adrenaline that activates G_s-proteins via β-adrenergic receptors. These G_s-proteins activates in turn adenylyl cyclase resulting in increased intracellular levels of cAMP that binds to the cyclic nucleotide-binding domain of the channels and thereby increases the $I_h/I_f/I_q$ current, see figure 6. The depolarization will be faster and the time between two action potentials will be shorter. The result will be among others increased heart rate.

2.3. Gating Mechanism of Three 6TM K^+ Channels

Gating mechanism is the mechanism by which the channel undergoes transitions between different states, opened, closed and inactivated. The transition between the different states is due to movement of three distinct structural moieties: the voltage sensor, the activation gate and the inactivation gate. The mechanism of three different 6TM K^+ channels, *Shaker*, HERG and HCN, will be explored in this section.

2.3.1. Gating Mechanism of the Shaker *K^+ Channel*

Shaker, as well as HERG and HCN, belongs to the family of voltage activated potassium channels. The voltage sensor of the *Shaker* K^+ channel is the S4 helix with its positively charged amino acids. These charged residues cause the S4 helix to move through the membrane at different voltages (Larsson *et al.*, 1996). At a resting potential of −70 to −80mV the S4 is retracted into the cell. Upon depolarization to more positive voltages S4 is moved outward in a series of steps (Baker *et al.*, 1998) and probably in a twist like motion (Cha *et al.*, 1999; Gleaner *et al.*, 1999). This displacement generates a gating current by carrying the basic residues outward across the membrane (Aggarwal & MacKinnon, 1996), see figure 7. Measurements have indicated that over ten charges must be translocated across the membrane in the outward movement to accomplish the resulting gating current (Bezanilla & Stefani, 1994). Surprisingly few S4 residues (at most five and only two charged) are buried in the membrane and are inaccessible to the aqueous solution on either side of the membrane when S4 is at it innermost position

(Baker *et al.*, 1998). Upon displacement of the sensor, these S4 basic residues move outward into the aqueous phase, whereas a segment containing three or four basic amino acids moves from the cytoplasmic side into the membrane and becomes inaccessible from either side. Together this, with the knowledge that each channel has four subunit and therefore four voltage sensors, equals 12 charges and explains the gating current.

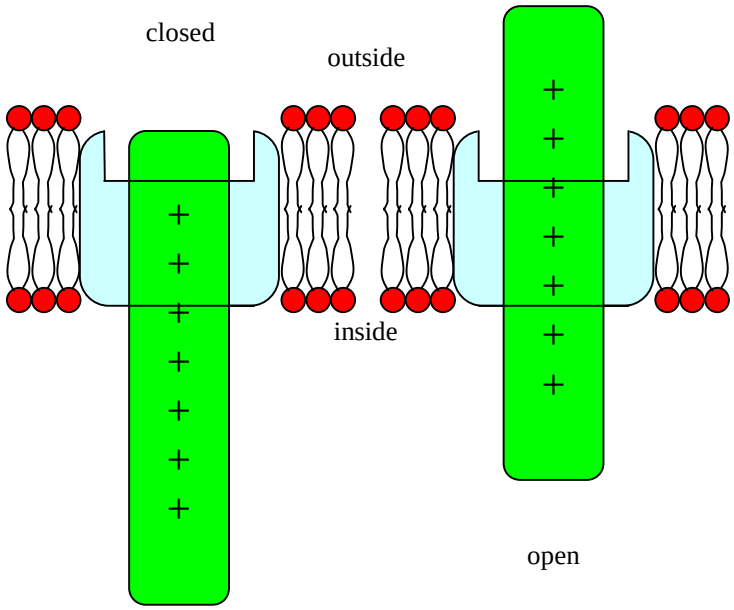

Figure 7. Transmembrane movement of the *Shaker* S4. The figure depict a region of protein around the S4 of a single subunit of the *Shaker* channel in the conformations associated with the channel closed and open states. Five residues span the distance between the intracellular and extracellular solution in the closed channel, leaving only two charged residues buried. When the channel opens, S4 moves outward. This movement of S4 closes the crevice leaving three charged amino acid buried. Modified from Baker *et al.*, 1998.

The outward movement of S4 at positive voltages is in some, yet unknown, way coupled to opening of the activation gate in the channel pore. The displacement of the sensor must lead to a conformational change of the channel that affects the activation gate. When the gate opens the channel can conduct ions through its pore.

The precise location of the activation gate is not yet fully known but experiments with state-dependent cysteine accessibility in S6 and structural data from the bacterial KcsA channel indicates that the gate is constituted of the criss-crossing of the S6 helices, see figure 8.

Another interesting feature of the *Shaker* channel, and also other K^+ channels, is that if the voltage is kept at positive potential the ion current will rapidly cease (in a few milliseconds) due to two different inactivation mechanism; N-type (ball-and-chain) and C-type inactivation.

The faster of the two mechanisms is the N-type mechanism that involves a N-terminal 'ball', first proposed by Armstrong and Bezanilla in 1977. Two types of experimental results indicate that this inactivation mechanism constitutes of an intracellular peptide sequence of the channel. The first was the finding that mild treatment with intracellular proteases could abolish the inactivation process (Armstrong *et al.*, 1973) while leaving the activation gating intact. This made it appear that a piece of the protein, important for inactivation, could be selectively removed. Genetically deletions of the first ~20 amino acids near the N-terminus of the *Shaker* channel was equally effective in removing the inactivation as pepsin treatment (Hoshi *et al.*, 1990). Furthermore, a soluble peptide containing the sequence of the first 20 amino acids could, if added intracellular, restore inactivation of the deletion-mutant channel (Zagotta *et al.*, 1990).

The peptide attached to the N-terminus of each channel subunit appears to act as an open channel blocker. Recovery from inactivation (interpreted as dissociation of the peptide from its binding site) can be speeded by an increase in extracellular K^+, as though K^+ ions entering the pore from the extracellular side can destabilize the bound peptide through repulsion. Another feature of this form of inactivation is that it exhibit the 'foot-in-door' effect: N-type inactivation tends to hold the activation gate open, as a consequence there is a current through the channel after return to negative voltages leading to recovery from inactivation (Demo & Yellen, 1991). It is clear that the 'ball' binds somewhere to the pore and thereby blocking the current through the channel, but exactly where in the pore this blocking is located is not fully elucidated.

Removal of the N-type inactivation peptide sequence of the *Shaker* K^+ channel does not prevent the ceasing of the current at positive voltages, though the current stops after a few seconds not milliseconds as with intact N-type inactivation. This lead to the discovery of another type of inactivation named C-type. This slower form of inactivation occurs by a mechanism distinct from the N-type. The pore blocker tetraethylammonium (TEA) interferes with N-type inactivation when applied intracellular but not extracellular, probably because of competition between TEA and the inactivation 'ball' (Choi *et al.*, 1991). C-type inactivation, exhibited by *Shaker* channels when N-type inactivation is disrupted, was not sensitive to intracellular TEA, but it was prevented by extracellular TEA binding. This indicates that C-type inactivation involves some changes at the extracellular mouth of the pore, see figure 8. Two lines of evidence implicate the selectivity filter of the K^+ channel as a participant in C-type inactivation gating: the substantial effects of permeant ions on the inactivation and large changes in selectivity sometimes associated with C-type inactivation (Yellen, 1998). Removing K^+ completely, both intra- and extracellular, allows C-type inactivation of *Shaker* channels to occur in milliseconds, whereas in elevated K^+ concentrations the process takes seconds. The open, non-inactivated state of the channel is stabilized by permeant ions like K^+ and Rb^+. Thus, occupancy of some ion site in the pore, capable of being filled by permeant ions, is sufficient to prevent or slow entry into the C-type inactivated state. The intimate relationship between C-type inactivation and the selectivity filter is also dramatically illustrated by the finding that the C-type inactivated state is actually capable of conducting Na^+, when K^+ is completely removed (Starkus *et al.*, 1997). So it appears that

C-type inactivation involves a very specific change in the selectivity filter, which is no longer capable of conducting K^+, though it is able to conduct other smaller ions, like Na^+.

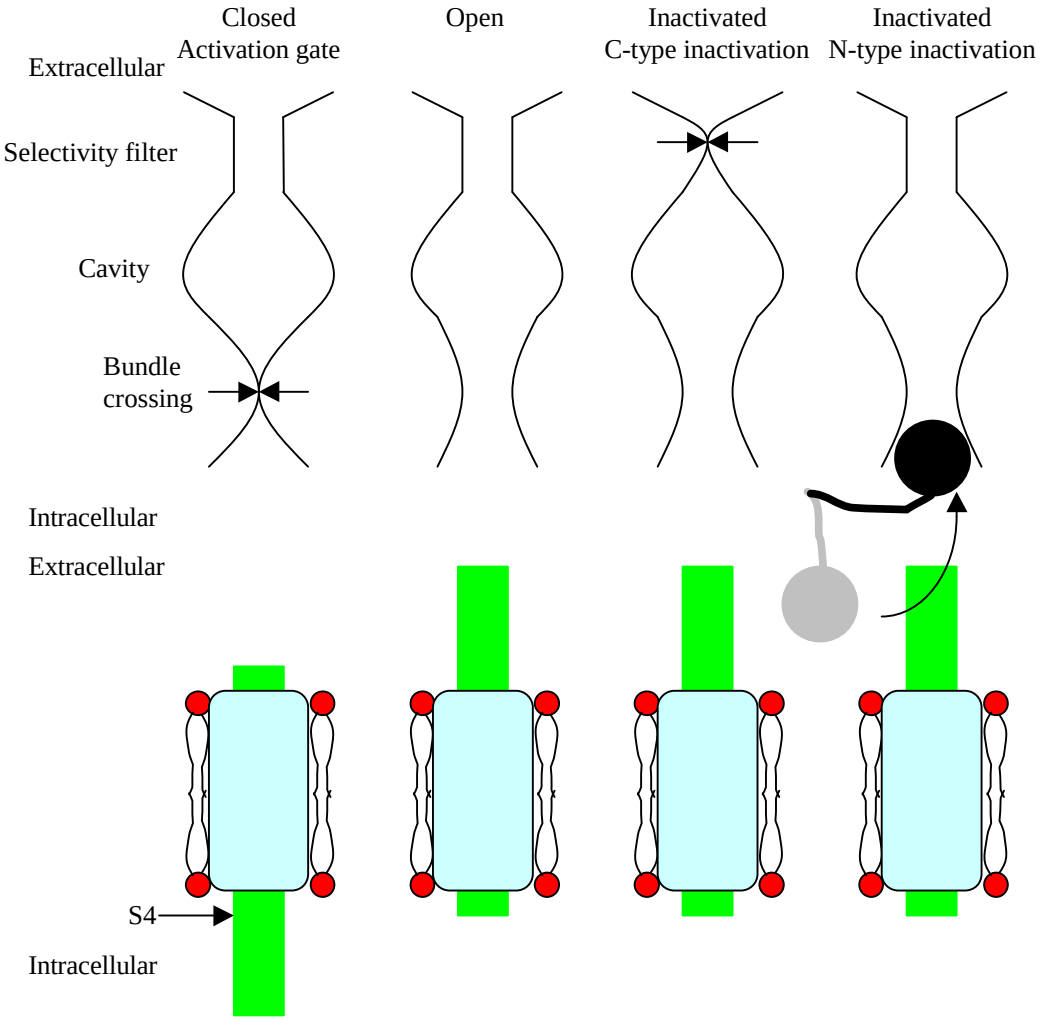

Figure 8. *Shaker* K^+ channel pores at closed, open and C- respective N-type inactivated states. The upper part of this cartoon summarizes the three types of gating motion that closes the transmembrane pore of K^+ channels at the different states. A full description is in the text. In the lower part one can see a schematic picture of the position of the voltage sensor, S4, at the different states. S4 is colored green whereas the rest of the channel is colored pale blue. Modified from Yellen, 1998.

The gating mechanism of *Shaker* can be summarized as in figure 9. Transitions along the y-axis in figure 9, corresponds to movement of the voltage sensor, whereas movement of the activation and inactivation gates can be found along the x- and z-axes. Stepping to

positive voltages from a resting potential of –70mV first leads to outward movement of the voltage sensor that triggers opening of the activation gate, resulting in an outward current. This current ceases after a short while due to closure of the inactivation gate. Stepping back to the resting potential first results in closure of the activation gate, then inward movement of S4 and opening of the inactivation gate, see the right part of figure 9. This scheme of transitions applies for *Shaker* channels lacking N-type inactivation, still undergoing C-type inactivation.

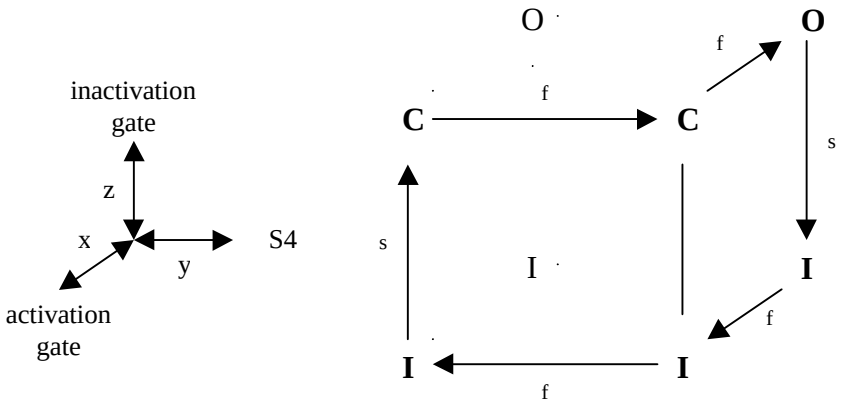

Figure 9. Schematic representation of the movement of the voltage sensor, activation gate and inactivation gate of *Shaker*. The axes of a coordinate system corresponding to the three different movements are displayed to the left. To the right the transition between the different states for *Shaker* is shown. C, O and I correspond to closed, open and inactivated states, whereas f and s correspond to fast respective slow transition. Stepping from the resting potential, -70mV, to positive voltages leads to an outward movement of the voltage sensor (C→C) that triggers opening of the activation gate (C→O). After a while in this open state the ion current stops due to closure of the inactivation gate (O→I). A step back to the resting potential results in closure of the activation gate, inward movement of the sensor and opening of the inactivation gate (I→I→I→C).

2.3.2. Gating Mechanism of the HERG K^+ Channel

The HERG K^+ channel is unusual in that it has the architectural plan of a 6TM voltage-gated channel, yet it exhibits rectification like that of the 2TM inward rectifier channels. Smith *et al.* (1996) have shown that the inward rectification of HERG is a result of a rapid voltage-dependent inactivation process that reduces conductance at positive potentials. The channel goes through the same sequence of states, closed↔open↔inactivated, as the *Shaker* channel, despite the large difference in rectification of the two channels. This is explained by an unusual slow activation gate and a fast inactivation gate. A positive voltage step from a resting potential of –70mV will, as in the case of *Shaker,* lead to an outward movement of the voltage sensor. This movement triggers opening of the activation gate, but before any ions can move through the channel the inactivation gate closes and blocks the pore. The result is a reduced

conductance at positive voltages. Stepping back to the resting potential leads to recovery from inactivation, that is opening of the inactivation, see figure 10. The channel pore is now open and ions can pass through, resulting in inward potassium current. After ~100ms the current stops due to closure of the activation gate. The gating mechanism is, in other words, the same as for the depolarization-activated *Shaker* channel. The disparity of the two channels is the kinetics of the activation and inactivation gates and this explains the differences in rectification and at what voltages the channels activate.

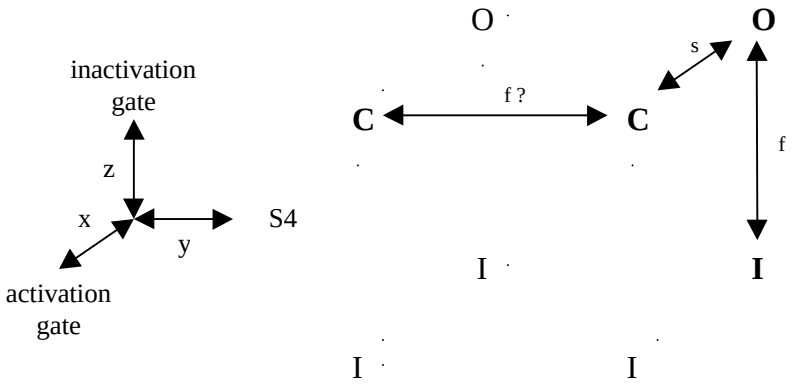

Figure 10. Gating mechanism of the HERG K^+ channel. The axes of a coordinate system corresponding to the three different movements are displayed to the left. To the right the transition between the different states for HERG is shown. C, O and I correspond to closed, open and inactivated states, whereas f and s correspond to fast respective slow transition. A step from the resting potential, -70mV, to positive voltages leads to an outward movement of the voltage sensor (C→C) and opening of the activation gate (C→O). This gate is unusually slow resulting in closure of the fast inactivation gate (O→I) before any currents can pass through the channel. Stepping back to the resting potential leads to opening of the inactivation gate (I→O) and currents can pass through the channel. This currents stops after a short while due to closure of the activation gate (O→C). S4 will then move into its buried position in the membrane (C →C).

Characterizing the mechanism of rectification has important implications for the pharmacology of HERG and its roll in the heart. The current through the channel resembles those that occur in the heart during generation of a premature beat (Smith *et al.*, 1996). This indicates that the channel might have an important roll in suppressing the generation of premature afterbeats. This theory is supported by the fact that patients lacking HERG currents, because of a genetic defect, show increased incidence of cardiac sudden death. Knowledge of the gating mechanism of HERG might be a key to, in the future, finding a cure for heart abnormalities caused by defects in HERG.

2.3.3. Gating Mechanism of HCN K^+ Channels

The gating mechanism of HCN channel is not yet fully understood. One idea, that was first given by Santoro *et al.*, 1998, is that the activation gating is shifted to negative potentials compared to depolarization-activated K^+ channels. This idea is supported by

experiments of Miller & Aldrich, 1996 on the *Shaker* K^+ channel, which normally activates rapidly and then, inactivates upon depolarization. The authors showed that point mutations in the voltage sensor shifts the activation gating to very negative potentials, well below the resting potential. This transformed the *Shaker* channel into a hyperpolarization-activated channel. At voltages near the resting potential, even though the activation gate of the mutant channel is in the open configuration, the channel is closed due to inactivation. Moderate hyperpolarization, which is not sufficiently negative to shut the activation gate, opens the channel by causing the inactivation gate to open. This could explain the behavior of most HCN channels cloned from mammals. They start to open at ~-70mV but the inward current does not cease even if you step to potentials of −130mV (Santoro *et al.*, 1998). The reason for this could be that the activation gating is shifted to very negative voltages so that the channels will not begin to close until you step to potentials more negative than −130mV. Regarding the activation gating, the HCN channel cloned from the sea urchin *Strongylocentrotus purpuratus*, SPIH, at a first glance look more like the HERG channel than the HCN channel. SPIH starts to activate at ~−25mV and the inward current begins to cease, after a few tens of milliseconds, already at 60mV (Gauss *et al.*, 1998). A large difference exists though; a depolarization step from the resting potential, −70mV, is not necessary before opening of SPIH at negative voltages as for HERG. To open the HERG channel at negative potential this pre-step to positive voltages is necessary to open the activation gate. So SPIH does not seem to have the same gating mechanism as HERG. Another theory about the gating mechanism of SPIH is that it behaves as Santoro *et al.*, 1998 proposed but with one exception: the activation gating is not shifted as far negatively as for the other HCN channels. The hypothesis that I worked with is that the gating mechanism of SPIH is opposite to that of *Shaker*: at positive voltages, when the sensor helix is in its outermost position, the activation gate of SPIH is closed not open, as for *Shaker*. A hyperpolarized step will lead to an inward movement of the voltage sensor, which will trigger opening of the activation gate and an inward current. After some tens of milliseconds the current stops due to closure of the inactivation gate. The opposite sequence of events takes place at a step back to positive voltages. First the inactivation gate opens and ions can once again pass through the channel but now in an outward direction. After a few milliseconds the currents stops due to closure of the inactivation gate and then the voltage sensor moves outward, see figure 11. This hypothesis fits well with the recordings done by Gauss *et al.*, 1998. Experiments with an inward rectifier found in plants, KAT1, supports this theory. Zei & Aldrich, 1998 have shown that the activation gate of KAT1 is closed when the voltage sensor is in its outermost position at positive potentials, that is opposite to the *Shaker* channel.

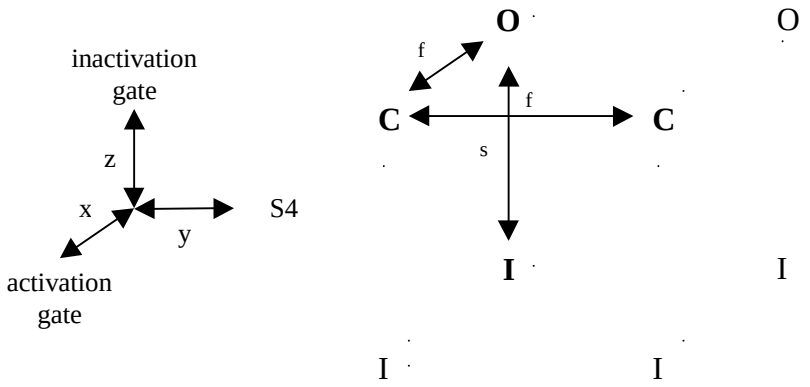

Figure 11. Hypothetical explanation for the gating mechanism of SPIH channels. The axes of a coordinate system corresponding to the three different movements are displayed to the left. To the right the transition between the different states for SPIH is shown. C, O and I correspond to closed, open and inactivated states, whereas f and s correspond to fast respective slow transition. A step from the resting potential, -10mV, to negative voltages leads to an inward movement of the voltage sensor (C←C) and opening of the activation gate (C→O). Ions can now pass through the channel until the inactivation gate closes (O→I) and the inward current stops. Stepping back to the resting potential leads to opening of the inactivation gate (I→O). Currents can once more move through the channel but now in an outward direction. This currents stops after a short while due to closure of the activation gate (O→C) and then the voltage sensor moves outward (C→C).

3. Materials and Methods

3.1. Solutions

Following solutions were used in the experiments, concentrations in mM.

	MBS (+ pyr and P/S)	1mM K^+	100mM K^+
NaCl	88	88	
KCl	1	1	89
$NaHCO_3$	2.4		
HEPES	15	15	15
$Ca(NO_3)_2 \bullet 4H_2O$	0.33		
$CaCl_2 \bullet 2H_2O$	0.41	0.4	0.4
$MgSO_4 \bullet 7H_2O$	0.82		
$MgCl_2 \bullet 6H_2O$		0.8	0.8
pH	7.6	7.4	7.4
	(+ 2.5mM pyruvate and 25µg/ml penicillin and streptomycin)		

1mM K^+ is used in electrophysiological experiments and 100mM K^+ in fluorescence measurements if not otherwise stated. Note that NaOH, for 1mM K^+, and KOH, for 100mM K^+, was used to adjust the pH leading to a final concentration of 99mM Na^+ for 1mM K^+ and 100mM K^+ for 100mM K^+.

3.2. Molecular Biology

cDNA of the SPIH channel, cloned into the plasmid pGEMHEnew was kindly given from Renate Gauss, Forschungszentrum Jülich (Jülich, Germany). Five different mutant channels were produced in which residues in the voltage sensor, S4 in figure 4, where mutated to cysteines. The four outermost positively charged residues and a serine in position 338 were changed, see figure 12. The mutant channels will from now on be called, R326C, K329C, R332C, K335C respective S338C. The letters are the one letter amino acid code and the numbers correspond to residue numbers in SPIH.

326-**R**AL**K**IL**R**FA**K**LL**S**LL**R**LL**R**LS**R**LM**R**-350

Figure 12. The voltage sensor, S4 in figure 4, of SPIH. The positively charged residues are in bold and the amino acids that were mutated into cysteines are colored red.

3.2.1. Site-Directed Mutagenesis

Site-directed mutagenesis was done by the use of Quik Change mutagenesis kit from Stratagene. The Quik Change site-directed mutagenesis method is performed using *PfuTurbo*™ DNA polymerase II and a thermal temperature cycler. The basic procedure utilizes a supercoiled double-stranded DNA vector with an insert of interest and two synthetic oligonucleotide primers, each containing the desired mutation, see figure 13. The oligonucleotide primers, each complementary to opposite strands of the vector, are extended during temperature cycling by the polymerase. Incorporation of the primers generates a mutated plasmid containing staggered nicks. Following temperature cycling, the product is treated with *Dpn I*. This endonuclease is specific for methylated and hemimethylated DNA and is used to digest the parental DNA template and to select for mutation-containing synthesized DNA. The nicked vector DNA, incorporating the desired mutations, is then transformed into Epicurian Coli® Xl1-Blue supercompetent cells.

The mutations were examined by DYEnamic™ ET terminator cycle sequencing, from Amersham Pharmacia Biotech.

3.2.2. Transcription

The DNA vectors were linearized with *Nhe I* followed by proteinase K treatment. Proteins were extracted with 1:1 phenol:chloroform, the linearized DNA was precipited with ethanol and then dissolved in RNase free water. cRNA was transcribed using T7 Ambion mMessage mMachine and template DNA was removed by DNase treatment. LiCl was used to precipitate the cRNA, which was then dissolved in RNase free water.

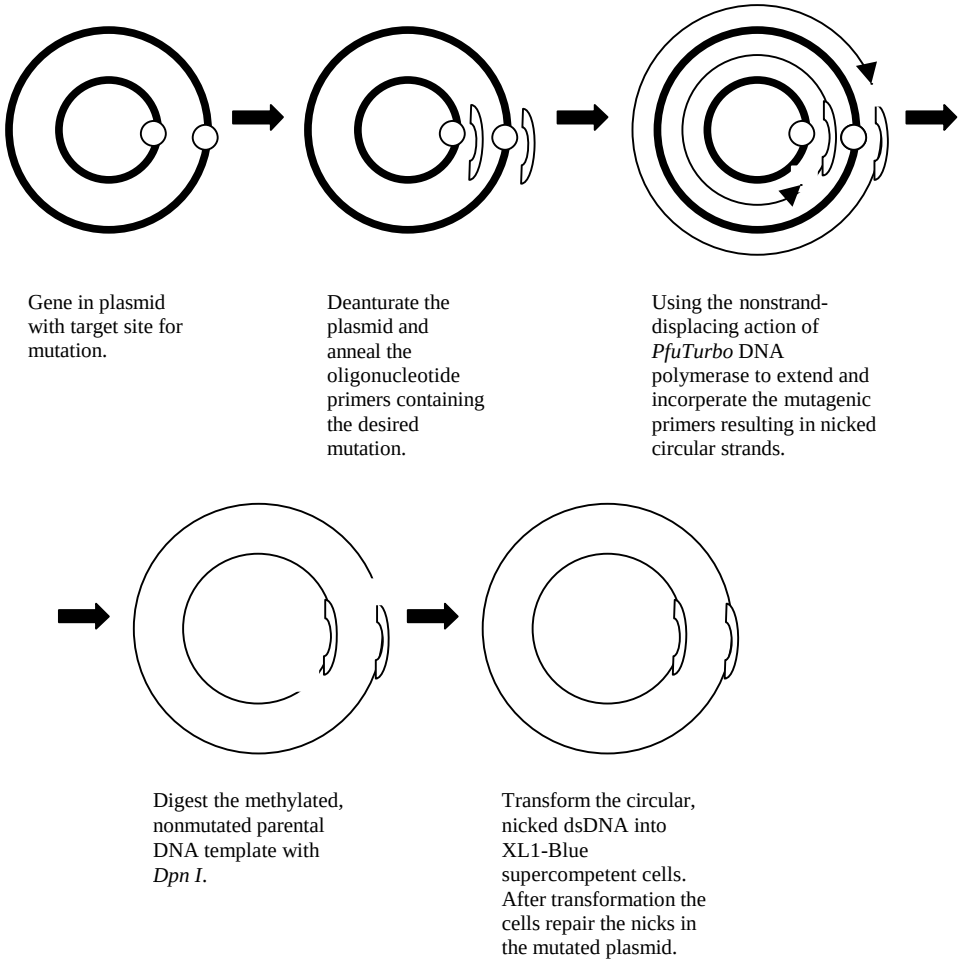

Figure 13. Overview of the Quik Change™ site-directed mutagenesis method.

3.3. Expression of SPIH Channels

50 nl cRNA at a concentration of ~1ng/µl was injected into stage V-VI oocytes from *Xenopus laevis* as described in Larsson *et al.*, 1996. The injected oocytes was maintained in MBS + pyr and P/S at 12°C (for two-electrode voltage clamp meassurements) or at 8°C (for voltage clamp fluorometry meassurements) 3-6 days before recordings were performed.

3.4. Electrophysiology

3.4.1. Two-Electrode Voltage Clamp

Two-electrode voltage clamp (TEVC) recordings were performed with 0.4-1.5 MΩ electrodes, filled with 3M KCl, using a Dagan CA-1B amplifier (Dagan Corporation). The voltage clamp was digitized and controlled by a Digidata-1200 board using the pCLAMP 8 software package (Axon Instruments). Data were filtered at 1kHz with a low pass Bessel filter. The holding potential was −10mV if not otherwise stated. The relative slow recovery of the channels forced me to use long interpulse intervals in my series of voltage-clamp steps, 30 s between voltage steps, to avoid accumulation of inactivation. All recordings were carried out at room temperature, 20-23 °C, in either high K^+ solutions, 100mM K^+, or in low K^+ solutions, 1mM K^+. Agents were applied continuously in the bath solution by a gravity-driven perfusion system. cAMP regulation is explored using forskolin treatment. The oocytes were incubated for 20 minutes in 10µM forskolin in MBS before TEVC recordings.

3.4.2. MTSET/MTSES Labeling

Solvent exposure of the inserted cysteines was assayed using irreversible covalent modification by the two membrane-impermeant thiol reagents [2-(trimethylammonium) ethyl]methanethiosulfonate bromide (MTSET) and sodium [(2-sulfonato ethyl)methanethiosulfonate] (MTSES). A 10-100mM stock solution of MTSET/MTSES dissolved in ice-cold recording solution was made, stored on ice and used to provide aliquots that were freshly diluted ~30s prior to perfusion. A new stock was made approximately every third hour. The robust effect of MTSET/MTSES modification for each S4 position studied enabled me to assay functionally if a particular position was exposed extracellularly and whether it was exposed in open and/or closed channels. The external accessibility was assayed with bath perfusion of oocytes under TEVC. The time course of channel modification was followed by recording the activation or inactivation time constants at a brief (100-900ms) hyperpolarized prepulse to −100mV prior application of the thiol chemicals.

3.5. Voltage Clamp Fluorometry

Two-electrode voltage clamp fluorometry was performed with 0.4-1.5 MΩ electrodes, filled with 3M KCl, using a Dagan CA-1B amplifier (Dagan Corporation), illuminated with a 300mW argon ion lamp, on a Nikon Diaphot 200 microscope, using a 20×0.75 n.a. fluorescence objective (Nikon). Photometry was performed with a Hamamatsu R-928 photomultiplier tube. The voltage clamp, photomultiplier and shutter were digitized and controlled by a Digidata-1320A board using the pCLAMP8 software package (Axon instruments). 100mM K^+ was used as bath solution. Oocytes were injected according to chapter 3.3. and stored at 8 °C for 2-3 days before blockage of extracellular cysteines with tetraglycine malemide (TGM), 1mM in MBS for one hour in room temperature. Oocytes were then incubated 15-17 hours in room temperature, in MBS + pyr and P/S, to permit expression of channels and incorporation in the plasma membrane. The channels were then labled with tetramethylrhodamine-5-malemide (TMR-5-M), 100µM, in 100mM K^+ for 30 minutes on ice. After extensive wash with MBS the oocytes were kept on ice in MBS + pyr and P/S. All fluorometry experiments were conducted with the R332C mutant channel.

4. Results and Discussion

4.1. Electrophysiological Measurements of SPIH wild-type and Mutant Channels

Both the SPIH wild-type channel and all the five mutant ones, R326C, K329C, R332C, K335C and S338C, where functionally expressed in oocytes and currents could be measured using TEVC. A typical recording is seen in figure 14. Down to the right in figure 14 the protocol of the recordings is found: from the holding potential -10mV steps to more negative voltages was conducted followed by a step to 50mV and then back to the holding potential.

For the wild-type channel one can first notice a very fast, faster than 10ms, voltage-dependent opening of the channel at the negative steps. After ~25ms at these negative voltages the inward current ceases probably due to inactivation. Stepping to 50mV leads to recovery from inactivation, resulting in a small outward current. As the channels deactivate, close, the current stops. The R326C, K329C and R332C mutations behave more or less the same. Of these three mutations only K329C inactivates at these voltages, but recordings down to −180mV, data not shown, indicates that the other channels also inactivates, though the transitions from closed to open and from open to inactivated states are shifted to more negative voltages compared to wild-type. Since the channels do not inactivate at the voltages in figure 14, the channels do not have to recover from inactivation at 50mV and therefore no increase in outward current is seen at this voltage. The K335C mutation deactivates much slower than the other channels, indicating that the lysine in position 335 might somehow be involved in closure of the activation gate.

Compared to the wild-type all mutant channels activates more slowly and at more negative potentials, see figure 15 and 16. In figure 15 the conductance for the wild-type and all mutant channels is plotted at different voltages. Mutating one of the four outermost positively charged amino acids in the voltage sensor will lead to a shift of the conductance curve to more negative voltages, resulting in a lower open probability of the mutant channels in the interval −10 to −70mV compared to wild-type. In figure 15 one can also see that mutating a serine to a cysteine, which is not a big change, does not lead to such a large shift of the conductance curve as mutating a charged residue to a cysteine.

The activation time constants at the steps from the holding potential to the different voltages in the interval −10 to −120mV are plotted in figure 16 for the mutant channels. The activation time constants for wild-type channels were too fast to be measured. All the mutant channels activated slower compared to wild-type, though the difference between wild-type and S338C was not that large. Thus, removing one of the four outermost positively charged residues of the sensor leads to a slower activation. This is probably a result of a slower movement of S4 in relation to changes in voltages. By having fewer positive charges the sensor responds slower to potential steps than if it had more charges.

Another explanation could be that the outer positive amino acids in S4 might interact with other residues in the channel. This interaction could be important for opening of the activation gate, for example by stabilizing the open conformation of the channel.

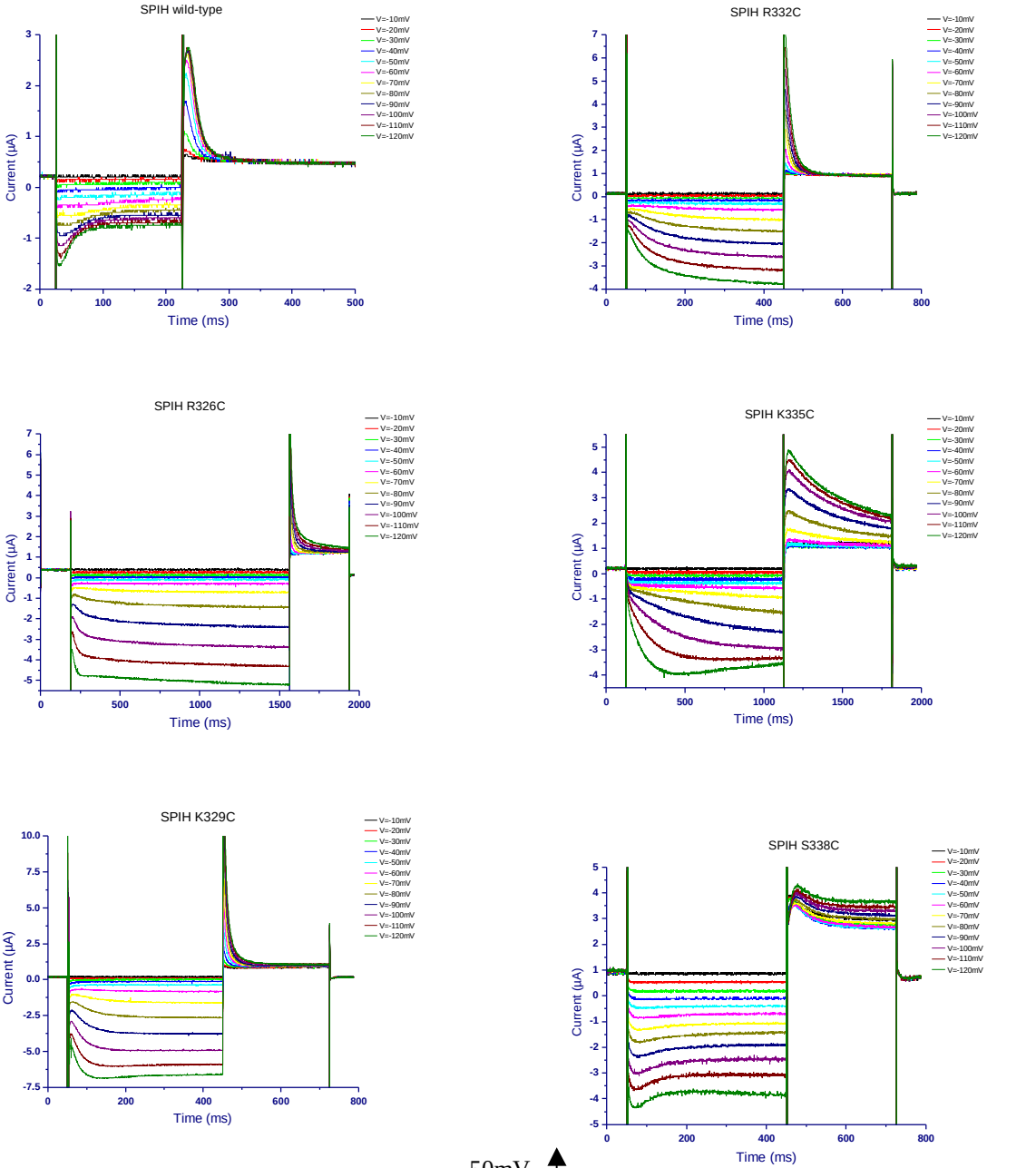

Figure 14. Two-electrode voltage clamp recordings of SPIH wild type and the five mutant channels (R326C, K329C, R332C, K335C and S338C) in 1mM K^+. The protocol used is seen down to the right. From a holding potential of –10mV steps to -120mV in 10mV increments was performed, followed by a step to 50mV and then back to the holding potential. Note the different scales of x-and y-axis.

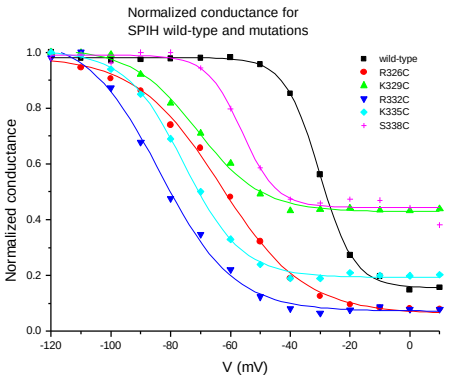

Figure 15. Normalized conductance for SPIH wild-type and the mutant channels at different voltages. The conductance is fitted with a Boltzmann function.

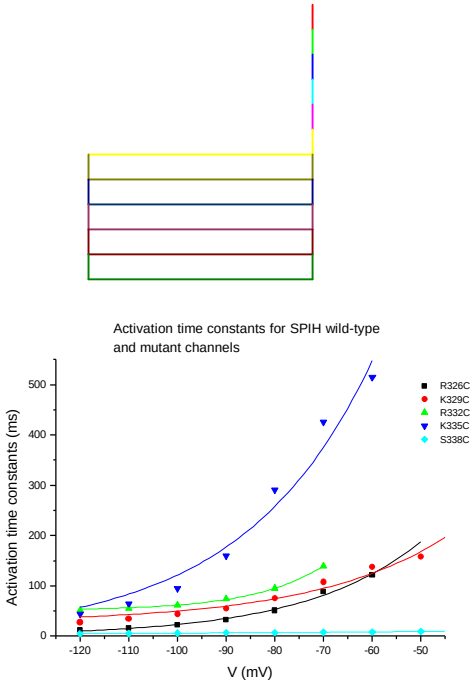

Figure 16. Activation time constants of the mutant channels at different voltages. The voltage dependence of activation is represented by an exponential fit to the experimental data.

4.2. Permeability

The inward current through SPIH and other HCN channels at negative potentials is a mixed current, consisting of both potassium and sodium ions. This differs from other groups of potassium channels that usually have much larger selectivity of K^+ over Na^+. In figure 17 the different permeability of K^+ and Na^+ of SPIH is explored. To the left a recording, according the protocol in figure 14, in low extracellular potassium, 1mM K^+, can be found and to the right the same recording is done but in high potassium, 100mM K^+.

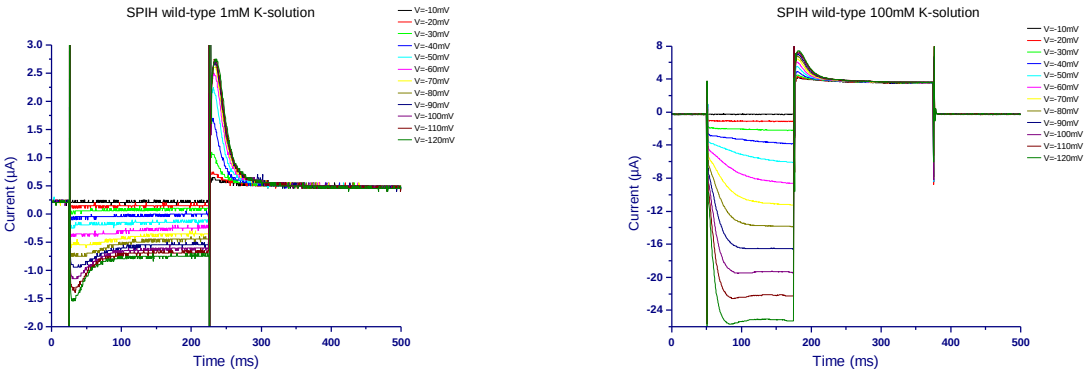

Figure 17. TEVC recordings of SPIH wild-type in low, 1mM K^+, and high, 100mM K^+, extracellular potassium solution. The same protocol as in figure 14 was used. Note the difference in scales of the y-axis.

The inward currents is much larger in high K^+, compared to low K^+, 15 times larger at ~-120mV. Another noticeble difference is that inactivation is not as pronounced in high K^+ as in low K^+ for the voltages in figure 17. Using Nernst equation, equation (1), the reversal potential for the two ions at 1mM K^+ or 100mM K^+ can be estimated.

$$Vx = \frac{RT}{zF} \ln \frac{[X]out}{[X]in} \quad (1)$$

V, reversal potential of ion x; R, gas constant; T, temperature in Kelvin; z, charge of x; F, Faradays constant and $[x]_{out/in}$, extracellular/intracellular concentration of ion x.
In 1mM K^+ the reversal potentials for K^+ respective Na^+ are, using $[K^+]_{in}$=100mM and $[Na^+]_{in}$=1mM, ~-115mV and ~115mV. This means that at a voltage of ~-115mV the potassium current through the channel is zero and the inward current is more or less exlusively due to the sodium ions. In high extracellular K^+, 100mM K^+, the reversal potential is 0mV for K^+ and the inward current consists of only K^+. This toghether with the recordings in figure 17 illustrates the different permeabilities of the two ions. If sodium ions constitute the major part of the current, it will be much smaller than if the current is carried by potassium ions. The permeability of K^+/Na^+ in SPIH is explored further in Gauss *et al.*, 1998.

4.3. cAMP regulation

The HCN channels, in the contrary to most voltage-gated potassium channels, have an intracellular cyclic nucleotide-binding domain. For several HCN channel the direct binding of cAMP results in an increased inward current due to a shift of the conductance curve to more positive voltages. In SPIH this shift in conductance has not been reported, instead the increase in current is a result of increased open probability and prevention from inactivation, figure 18 illustrates this. In this figure the same recordings as to the left in figure 17, 1mM K^+, has been conducted but after forskolin treatment. Forskolin is a chemical that, applied extracelluarly, leads to increased intracellular levels of cAMP. As can been seen in the figure the current is ~20 times larger after, figure 18, than before, left in figure 17, forskolin treatment. Another noticeable difference is that the channels seem unable to inactivate at the voltages of the recordings. Binding of cAMP to the cyclic nucleotide-binding domain must lead to some conformational change of the channel that prevents the inactivation gate from closing at these voltages. The mechanism of this phenomenon is not yet known.

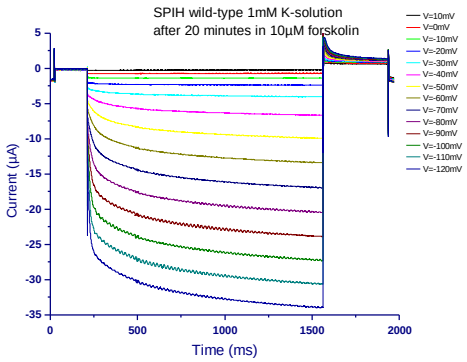

Figure 18. TEVC recordings of SPIH wild-type in 1mM K^+ after forskolin treatment (10µM in 20 minutes). The same protocol as in figure 14 was used.

4.4. Transmembrane Movement of the Voltage Sensor of SPIH Channels

To find out the position of the voltage sensor, S4, of SPIH at different voltages the two charged membrane impermeant reagents MTSET, posively charged, and MTSES, negatively charged, were used. These chemicals are able to bind to the voltage sensor by forming disulphid-bridges with the introduced cysteines. The idea was to apply the chemicals at either 50mV or −100mV to the outside of the oocytes and follow the binding of MTSET/MTSES to the cysteines of S4. If you follow the mutant residues in S4 from the outside towards the inside, at some position there will be a difference in binding of the chemicals at the two different voltages, that is there is a state dependent accessibility of the introduced cysteine. From such recordings the position of S4 relative the membrane at the different voltages is given and from this knowledge the movement of the voltages sensor can be explained.

Figure 19 shows that binding of MTSET or MTSES cause a shift in the conductance curve. Binding of MTSET to position 332C should shift the conductance curve to more positive voltages, that is towards wild-type. The reason for this is that by binding MTSET to 332C a positive charge is brought back to this postion. Changing the arginine of this postion to a cysteine leads to a negative shift in conductance curve and by putting back the positive charge in the form of MTSET the conductance curve is shifted back towards wild-type. The curve is not, as seen in figure 19, shifted back to the same position as wild-type. This could be due to incomplete coupling, so that MTSET does not bind to every voltage sensor per channel, remember that there is four S4 per SPIH channel. Another explanation could be the difference in size between an arginine and cysteine-MTSET, which might influence the open probability of the channel. Binding of the negatively charged MTSES should lead to the opposite behavior compared to MTSET, that is a shift in conductance to more negative voltages. This is seen for K335C in figure 19, where MTSES binding leads to a −5mV shift in the conductance curve.

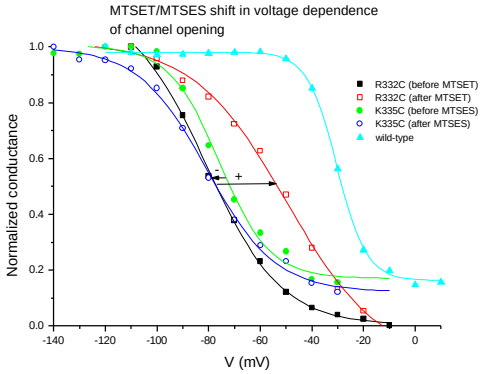

Figure 19. MTSET/MTSES induced shift in the conductance of R332C and K335C. 100µM of the reagents were applied according the protocol in figure 20 for 6 minutes. + shift caused by MTSET, - shift caused by MTSES.

As an indication of MTSET/MTSES binding the activation or inactivation time constants at a short prepulse to –100mV, see figure 20, were used. Labeling with the two thiol compounds followed a monoexponential time course and was concentration dependent, see figure 20.

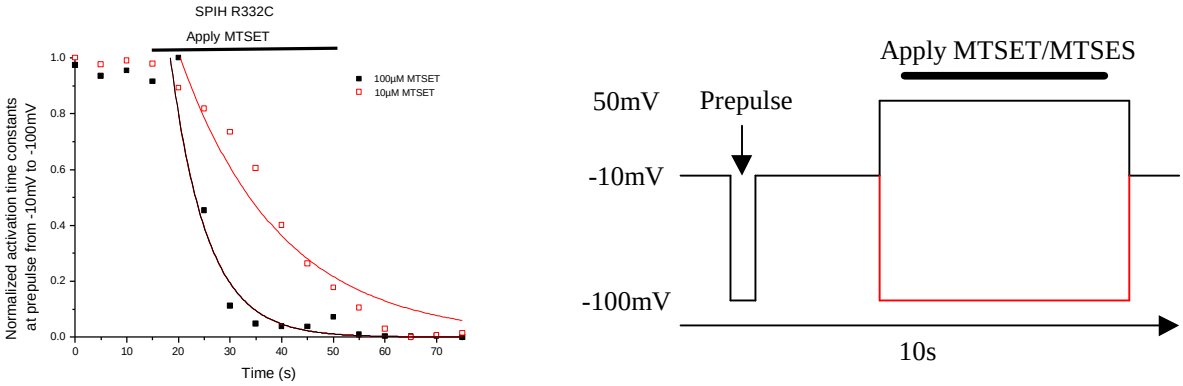

Figure 20. To the left binding of MTSET to the cysteine of position 332 at V=50mV, can be followed at to different concentrations, 10 and 100µM MTSET. The protocol of MTSET/MTSES application is seen to the right indicating the two different voltages during application, 50mV respective –100mV. The time constants have been fitted with a monoexponential curve. The two chemicals were applied during 5s per episode (30s between two episodes). As an indication of MTSET/MTSES binding the activation and inactivation time constants at a prepulse to –100mV, was used.

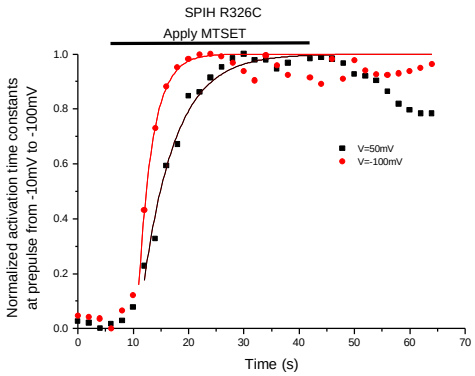

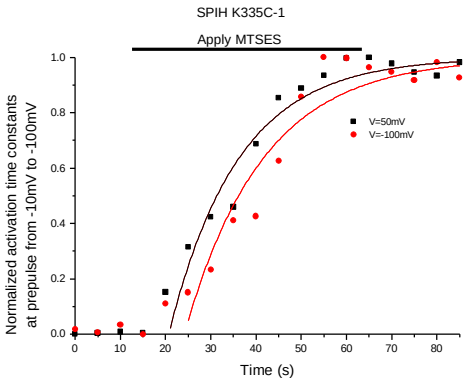

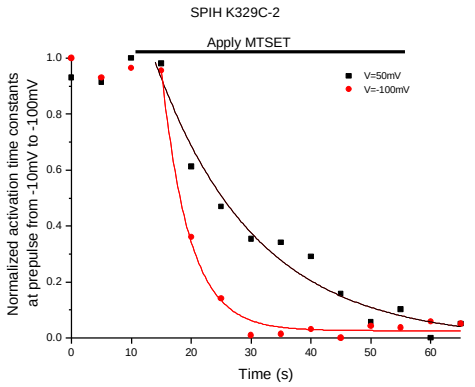

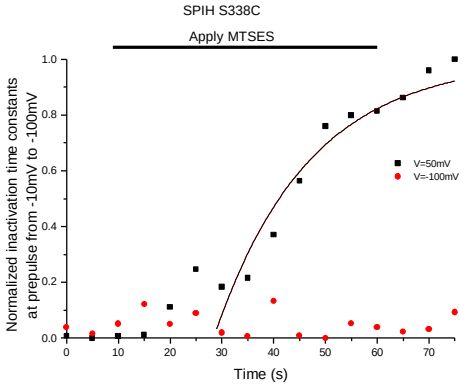

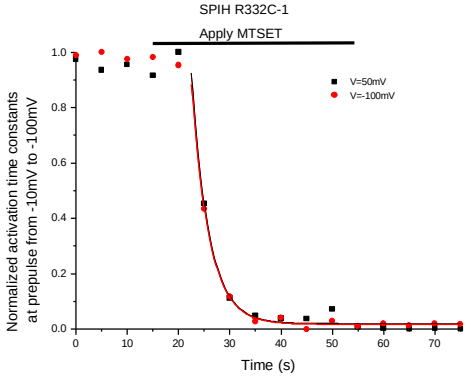

Figure 21. State-dependent accessibility of the cysteine mutations in the voltage sensor. Binding of 100µM MTSET/MTSES is followed at the two different voltages in figure 20. Application of the thiol reagents according the protocol in figure 20. The data has been normalized before plotting and fitted with a monoexponentail curve. Each plot is a average of five recordings.

To find out the state-dependent accessibility of the introduced cysteines in the voltage sensor, MTSET/MTSES was applied at two different voltages 50mV and −100mV according the protocol in figure 20. The result of MTSET/MTSES binding can be seen in figure 21. For the four outermost cysteines in S4 there is not any difference in reaction rate at the two potentials, so these residues are as accessible to the outside at −100mV as at 50mV. Binding of MTSET to K329C seems to be slower at 50mV than at −100mV according figure 21. The same kind of experiment was performed for this mutation but in 10µM MTSET. At this concentration the reaction rate was the same for the two voltages and the binding curves coincided as for the R326C, R332C and K335C mutants. The reason for the difference in reaction rate in 100µM between 50mV and −100mV is probably due to some problems in the recordings and this position should be as accessible to the outside at 50mV as in −100mV. Position 338 shows a different behavior in reaction rate compared to the other four cysteines: MTSES can only bind at 50mV but not at −100mV. In other words position 338C proves to have a state-dependent accessibility to the extracellular side.

The results from the MTSET/MTSES experiments can be summarized in the cartoon in figure 22. At −100mV, when the SPIH channels are open, position 326 to 335 are accessible to the outside whereas residue 338 is buried in the membrane or in the rest of the channel and is inaccessible from the outside. A step to 50mV will lead to an outward movement of the voltage sensor and closure of the channel. At this potential all residues 326-338 are now accessible from the outside. The reaction rates to residue 335 at V=−100mV and at 338 at V=50mV are three times slower compared to the other more outward cysteines, implying that these amino acids are partially blocked at respective voltage. The residues could be slightly buried in the membrane or in the rest of the channel so that the thiol compounds have difficulties in binding to the cysteines. The local environments of the cysteines are different which might result in different reactivity of the cysteines and/or a tendency to repel/attract the thiol reagents. This could be another explanation for the difference in reaction rate between 335 and 338 compared to the other positions.

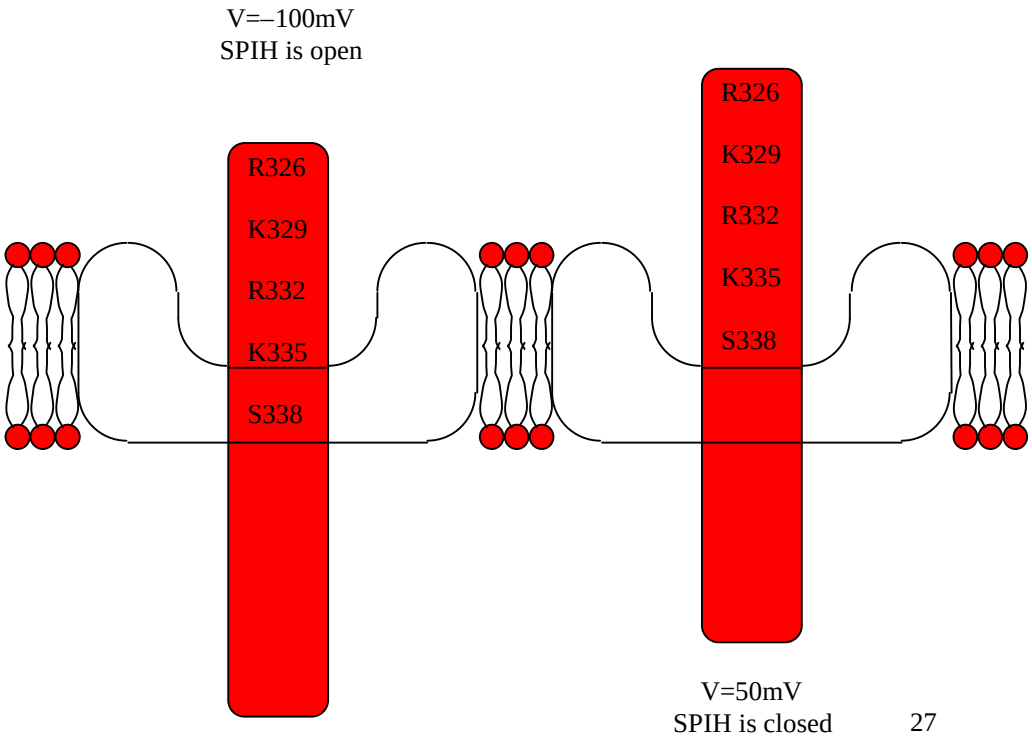

Figure 22. Cartoon showing the transmembrane movement of the voltage sensor in SPIH. At a voltage of −100mV, when the SPIH channel is open, the voltage sensor is positioned far in the membrane and residue 338 becomes inaccessible from the outside. Stepping to 50mV leads to outward movement of S4 and closure of the channel. At this potential all the residues 326 to 338 are accessible to the outside.

Conclusively, at negative voltages the voltage sensor is positioned down in the membrane and stepping to positive potentials leads to an outward movement of the sensor helix. These results are consistent with similar experiments on the *Shaker* K^+ channel (Larsson *et al.*, 1996), but none has, so far, published any data on the movement of a HCN voltage sensor. One big difference between the experiments with *Shaker* and HCN is that at positive voltages, when the sensor is in its outermost position, the *Shaker* channel is open whereas HCN is closed. Stepping to negative voltages leads to an inward movement of the sensor that triggers closure of the activation gate for *Shaker* and opening of the activation gate for HCN.

4.5. Voltage Clamp Fluorometry

To correlate the movement of the voltage sensor to the opening of the channel, voltage clamp fluorometry experiments were conducted. In these experiments a fluorophore, TMR-5-M, was connected to the voltage sensor in SPIH via a bond between the malemide group in TMR-5-M and one of the introduced cysteines in S4. The fluorescence of the fluorophore is sensitive to its local environment. In this technique changes in fluorescence can be followed at the same time as you measure currents through the channels. The idea is that by measuring the fluorescence and the current at different voltages, a correlation between the sensor movement and opening of the channel could be elucidated. In figure 23 the fluorescence and current steps to two different voltages is shown, from the holding potential to –30mV respective –100mV.

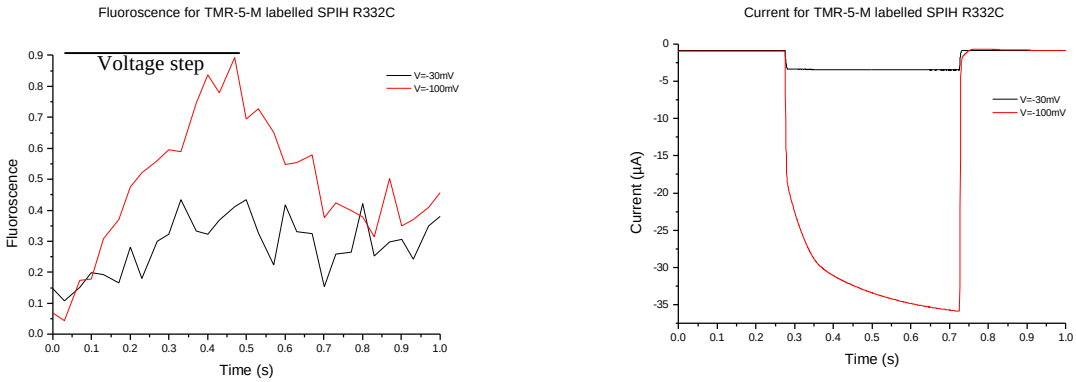

Figure 23. Voltage clamp fluorometry measurements. Down to the right the protocol used can be found. Up the fluorescence, to the left, and the current, to the right can be seen. The fluorescence data is a average of four recordings.

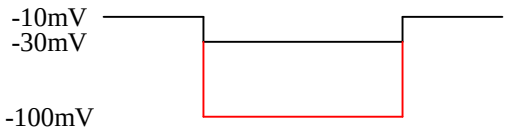

The fluorescence is normalized to the maximum fluorescence at V=−140mV. At the step to −30mV a relative small change in fluorescence is seen whereas no change in current could be measured. The inward current seen for V=−30mV in figure 23 is due to leakage current that has not been subtracted in this figure. If one apply a larger negative step, to −100mV, there is a large change in fluorescence and in current. Figure 23 indicates that there first is a change in fluorescence if you make a small negative step from the holding potential, but no change in current. Stepping further to negative voltages leads to a larger change in fluorescence and an inward current is measured. In figure 24 both the fluorescence and the conductance is plotted for different voltages.

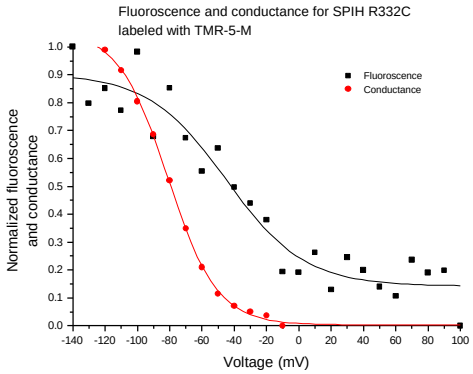

Figure 24. Fluorescence and conductance for SPIH R332C labeled with TMR-5-M. The fluorescence at each voltage is a mean of four different measurements and is expressed as the sum of the fluorescence during the voltage step. Both the fluorescence and conductance has then been normalized to respective maximum and fitted with Boltzmann functions.

What one first can notice is that stepping from the holding potential to more positive voltages does not change the fluorescence. Two different explanations exist for this phenomenon. The voltage sensor might not move any further if you step to positive voltages from −10mV. The sensor is then already in its outermost position at the holding potential. Another explanation could be that the sensor actually moves if you step to more positive potentials but this movement does not change the local environment of the flourophore. The flourophore could be positioned in the extracellular solution at −10mV and does not really interact with atoms from the channel. If the sensor is moved further outward the flourophore will be in more or less the same environment as in the position at −10mV.

A small step to more negative voltages from the holding potential results in a change in fluorescence but hardly any change in conductance. This indicates that the voltage sensor has moved inward, but the movement is not enough to open the activation gate, so no ions can pass through the channel yet. Stepping to more negative voltages will lead to a larger change in fluorescence and an increase in conductance. The sensor has now moved enough to trigger opening of the activation gate and currents through the channel can be measured. At potentials more negative than ~-90mV the fluorescence does not change, indicating that S4 of TMR-5-M labeled R332C is in its innermost position at that voltage.

5. Conclusions

The experiments with the charged thiol compounds, MTSET/MTSES, indicate that there is a voltage dependent movement of the sensor of the SPIH channel.

At positive voltages S4 is in its outermost position and the channel is closed. At these potentials residues 326 to 338 in the sensor are accessible to the extracellular side. Stepping to negative potentials leads to an inward movement of the voltage sensor that triggers opening of the activation gate, resulting in an inward current. When S4 is in this position residue 338 becomes buried in the membrane or in the rest of the channel, and is inaccessible to the outside. The movement of the sensor is not that large because residues 326 to 335 are still accessible to the extracellular side.

To find out how much the sensor moves one has to mutate more residues in S4 and measure accessibility from not only the extracellular but also the intracellular side of the membrane. To get a more accurate picture of the movement of S4 intracellular accessibility should be analyzed with 338C and preferable with new mutations (341C, 344C and so on). If one conduct such experiments one should find some residues that are accessible to the inside, but not the outside, at both voltages and some amino acids that are accessible to the inside at −100mV but not at 50mV. It might also be possible to find residues that are inaccessible to both the intracellular and extracellular sides at one of the potentials but becomes accessible if you step to the other one, see Larsson*et al.*, 1996. These results demonstrate the close relationship between the HCN channels and other voltage-gate K^+ channels, such as the Shaker, a depolarized-activated K^+ channel. Both groups of channels are activated by changes in voltages and these changes result in the movement of the sensor helix, S4.

The idea with the fluorescence experiments was to correlate the movement of the voltage sensor to the opening of the channel. The change in fluorescence of the S4 immobilized flourophore should change during steps to more negative voltages when the channel opens.

The voltage clamp fluorometry recordings in figure 23 shows that a small negative voltage step leads to a change in fluorescence due to an inward movement of the voltage sensor, but no current is recorded. This movement of S4 is probably not large enough to open the activation gate. Another explanation could be that all four or at least more than one of the voltage sensors must move for the channel to open. At the small step, from −10mV to −30mV, maybe only one or some of the sensors have moved and therefore the channel can not open. A larger negative voltage step results in both a change in fluorescence and an inward current. The movement of S4 is now sufficient to open the activation gate or all the voltage sensors have moved inward so that the channel now can open. The fluorometry experiments indicate that at a negative voltage step the sensor is first pulled into the membrane and only then can the channel open. Thus this inward movement of S4 must precede opening of the activation gate.

The idea with this master's degree project was to characterize the gating mechanism of the HCN channel SPIH. Knowledge of the gating mechanism of the HCN channel is important since the channels are involved in fundamental process in living organism such as respiratory and cardiac rhythms. The molecular characterization of these channels can be a key to identifying genetic alterations that may lead to cardiac arrhythmias, epilepsy and neurological disorders and also provide a new tool for the discovery of pharmacological agents that might find therapeutic niches related to cardiac and neurological diseases.

The working hypothesis was that the gating mechanism of SPIH was opposite to that of the well-characterized *Shaker*, a depolarization-activated K^+ channel. At positive voltages S4 of SPIH is in an outward position and the activation gate is closed. Stepping to negative voltages leads to an inward movement of the sensor, which, if the sensor is pulled enough into the membrane, will trigger opening of the activation gate, resulting in an inward, mixed K^+/Na^+ current. The current stops after a short while due to closure of the inactivation gate. Stepping back to positive voltages leads to opening of the inactivation gate, recovery from inactivation. Now the channel once more is open and a small outward current can be recorded before the activation gate closes and the current stops, deactivation. As a final step the voltage sensor is moved outward, see figure 25.

Inward movement of S4.

Opening of the activation gate.

Closure of the inactivation gate.

Opening of the inactivation gate.

Closure of the activation gate.

Outward movement of S4.

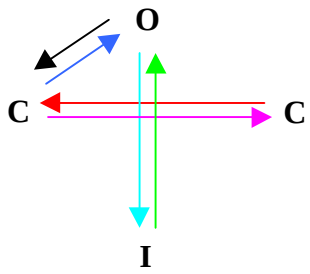

Figure 25. Schematic drawing of the hypothesized gating mechanism of SPIH. Color coding of the text corresponds to transitions, represented by arrows. C, O and I corresponds to closed, open and inactivated states. For clarification see text.

The inactivation mechanism of SPIH or any other HCN channel is not yet known. It is possible that a similar mechanism as in *Shaker*, N-type and/or C-type inactivation, is responsible for inactivation in SPIH.

Although the experimental data in of the project are not a proof of this gating theory, they support it. More experiments have to been performed before a deeper insight in the mechanism of HCN channels is elucidated, but this project is a first step in the right direction.

6. Acknowledgements

I would like to thank my supervisor Peter Larsson and examiner Fredrik Elinder for always being there for me and answering my questions with grate patience. I also would like to thank Roope Männikkö for his help with the molecular work and fluorescent experiments, and Peter Århem and Johanna Nilsson for pleasant company in the lab. Thanks also to Monika Bredmyr for showing me round in the lab, Peter Löw for letting me use the autoclave equipment and Tommy Nord for constructing my measuring chamber and finally Lars Flemström for his help with computers that suddenly malfunction. Lastly I would like to thank the rest of the people at the department of Neuroscience for making this a pleasant and interesting time. I will remember the interesting lunch seminars and the crayfish party although I did not enjoy the lemon flavored absolute ethanol.

7. References

Aggarwal, S. K., and MacKinnon, R. Contribution of the S4 segment fo gating charge in the *Shaker* K^+ channel. *Neuron* **16**, 1169-1177 (1996)

Armstrong, C., M. and Bezanilla, F. Inactivation of the sodium channel. II. Gating current experiments. *J. Gen. Physiol.* **70**, 567-590 (1977)

Armstrong, C. M., Bezanilla, F., and Rojas, E. Destruction of sodium conductance inactivation in squid axons perfused with pronase. *J. Gen. Physiol* .**62**, 375-391 (1973)

Baker, O. S., Larsson, H. P., Mannuzzu, L. M., and Isacoff, E. Y. Three transmembrane conformations and sequence-dependent displacement of the S4 domain in *Shaker* K^+ channel gating. *Neuron* **20**, 1283-1294 (1998)

Beaumont, V., and Zucker, R. S. Enhancement of synaptic transmission by cyclic AMP modulation of presynaptic Ih channels. *Nat. Neurosci.* **3**, 133-141 (2000)

Bezanilla, F., and Stefani, E. Voltage.dependent gating of ionic channels. *Annu. Rev. Biophys. Biomol. Struct.* **23**, 819-846 (1994)

Cha, A., Snyder, G. E., Selvin, P. R., and Bezanilla, F. Atomic scale movement of the voltage-sensing region in a potassium channel measured via spectroscopy. *Nature* **402**, 809-813 (1999)

Choi, K. L., Aldrich, R. W., and Yellen, G. Tetraethylammonium blockade distinguishes two inactivation mechanisms in voltage-activated K^+ channels. *Proc. Natl. Acad. Sci. USA* **88**, 5092-5095 (1991)

Clapham, D. E. Not so funny anymore: pacing channels are cloned. *Neuron.* **21**, 5-7 (1998)

Curran, M. E., Splawski, I., Timothy, K. W., Vincent, G. M., Green, E. D., and Keating, M. T. A molecular basis for the cardiac arrhythmia: HERG mutations cause long QT syndrome. *Cell* **80**, 795-803 (1995)

Dascal, N., Schreibmayer, W., Lim, N. F., Wang, W., and Chavkin, C. Atrial G protein-activated K^+ channel: expression cloning and molecular properties. *Proc. Natl. Acad. Sci. USA* **90**, 10235-10239 (1993)

Dekin, M. S. Inward rectification and its effects on the repetitive firing properties of bulbospinal neurons located in the ventral part of the nucleus tractus solitarius. *J. Neurophysiol.* **70**, 590-601 (1993)

Demo, S. D., and Yellen, G. The inactivation gate of the *Shaker* K^+ channel behaves like an open-channel blocker. *Neuron* **7**, 743-753 (1991)

DiFrancesco, D. Pacemaker mechanisms in cardiac tissue. *Annu. Rev. Physiol.* **55**, 455-472 (1993)

Doyle, D. A., Morais Cabral, J., Pfuetzner, R. A., Kuo, A. Gulbis, J. M., Cohen, S. L., Chait, B. T., and MacKinnon, R. The structure of the potassium channel: molecular basis of K^+ conduction and selectivity. *Science* **280**, 69-76 (1998)

Gauss, R., Seifert, R., and Kaupp, B. Molecular identification of a hyperpolarization-activated channel in sea urchin sperm. *Nature* **393**, 583-587 (1998)

Glauner, K. S., Mannuzu, L. M., Gandhi, C. S., and Isacoff, E. Y. Spectroscopic mapping of voltage sensor movement in the *Shaker* potassium channel. *Nature* **402**, 813-817

Ho, K., Nichols, C. G., Leder, W. J., Lytton, J., and Vassilev, P. M. Cloning and expression of an inwardly rectifying ATP-regulated potassium channel. *Nature* **362**, 31-38 (1993)

Hoshi, T, Zagotta, W. N., and Aldrich, R. W. Biophysical and molecular mechanisms of *Shaker* potassium channel inactivation. *Science* **250**, 533-538 (1990)

Ishii, K., Yamagashi, T., and Taira, N. Cloning and functional expression of a cardiac inward rectifier K^+ channel. *FEBS Lett.* **338**, 107-111 (1994)

Kubo, Y., Baldwin, T. J., Jan, Y. N., and Jan, L. Y. Primary structure and functional expression of a mouse inward rectifier potassium channel. *Nature* **362**, 127-133 (1993)

Kriksunov, I. "Structures solved by MacCHESS", 1998 http://www.chess.cornell.edu/MacCHESS/MacCHESS_publications/image_gallery_98.html (27 Nov. 2000)

Larsson, H. P., Baker, O. S., Dhillon, D. S., and Isacoff, E. Y. Transmembrane movement of the *Shaker* K^+ channel S4. *Neuron* **16**, 387-397 (1996)

Liman, E. R., Hess, P., Weaver, F., and Koren, G. Voltage-sensing residues in the S4 region of a mammalian K^+ channel *Nature* **353**, 752-726 (1991)

Littleton, J. T., and Ganetzky, B. Ion channel and synaptic organization: analysis of the *Drosophila* genome. *Neuron* **26**, 35-43 (2000)

Ludwig, A., Zong, X., Jeglitsch, M., Hofmann, F., and Biel, M. A family of hyperpolarization-activated cation channels. *Nature* **393**, 587-591 (1998)

Ludwig, A., Zong, X., Hofmann, F., and Biel, M. Structure and function of cardiac pacemaker channels. *Cell. Physiol. Biochem.* **9**, 179-186 (1999)

Maccaferri, G., and McBain, C. J. The hyperpolarization-activated current (I_h) and its contribution to pacemaker activity in rat CA1 hippocampal stratum orients-alveus ineterneurons. *J. Physiol. (London)* **497**, 119-130 (1996)

MacKinnon R Determination of the subunit stoichiometry of a voltage-activated potassium channel. *Nature* **350,** 232-235 (1991)

McCormick, D. A., and Bal, T. Sleep and arousal: thalamocortical mechanisms. *Annu. Rev. Neurosci.* **20**, 185-215 (1997)

Miller, A. G., and Aldrich, R. W. Conversion of a delayed rectifier K^+ channel to a voltage-gated inward rectifier K^+ channel by three amino acid substitutions. *Neuron* **16**, 853-858 (1996)

Miller, C. An overview of the potassium channel family. *Genome Biology* **1**, 1-5 (2000)

Nichols, C. G., and Lopatin, A. N. Inward rectifier potassium channels. *Annu. Rev. Physiol.* **59**, 171-191 (1997)

Papazian, D. M., Timpe, L. C., Jan, Y. N., and Jan, L. Y. Alteration of voltage-dependence of *Shaker* potassium channel by mutations in the S4 sequence. *Nature* **349**, 305-310 (1991)

Papazian, D. M., Shao, X. M., Seoh, S. A., Mock, A. F., Huang, Y., and Wainstock, D. H. Electrostatic interactions of S4 voltage sensor in *Shaker* K^+ channel. *Neuron* **6**, 1293-1301 (1995)

Perier, F., Radeke, C. M., and Vendenberg, C. A. Primary structure and characterization of a small-conductance inwardly rectifying potassium channel from human hippocampus. *Proc. Natl. Acad. Sci. USA* **91**, 6240-6244 (1994)

Santoro, B., Liu, D. T., Yao, H., Bartsch, D., Kandel, E. R., Siegelbaum, S. A., and Tibbs, G. R. Identification of a gene encoding a hyperpolarization-activated pacemaker channel of brain. *Cell* **93**, 717-729 (1998)

Santoro, B., and Tibbs, G. R. The HCN gene family: molecular basis of the hyperpolarization-activated pacemaker channels. *Ann. NY Acad. Sci.* **868**, 741-764 (1999)

Smith, P. L., Baukrowitz, T, and Yellen, G. The inward rectification mechanism of the HERG cardiac potassium channel. *Nature* **379**, 833-836 (1996)

Starkus, J. G., Kuschel, L., Rayner, M. D., and Heinemann, S. H. Ion conduction through C-type inactivated *Shaker* channels. *J. Gen. Physiol.* **110**, 539-550 (1997)

Yellen, G. The moving parts of voltage-gated ino channels. *Quart. Rev. Biophys.* **31**, 239-295 (1998)

Zagotta, W. N., Hoshi, T., and Aldrich, R. W. Restoration of inactivation in mutants of *Shaker* K^+ channels by a peptide derived from ShB. *Science* **250**, 568-571 (1990)

Zei, P. C., and Aldrich, R. W. Voltage-dependent gating of single wild-type and S4 mutant KAT1 inward rectifier potassium channels. *J. Gen. Physiol.* **112**, 679-713 (1998)